Pump-and-probe study in $LaMnO_3$ thin films

H. Tamaru,[1] K. Ishida,[2] N. Ogawa,[1] Y. Kubo,[2] and K. Miyano[1,3,*]
[1]*Research Center for Advanced Science and Technology (RCAST), The University of Tokyo, Tokyo 153-8904, Japan*
[2]*Department of Applied Physics, The University of Tokyo, Tokyo 113-8656, Japan*
[3]*CREST, Japan Science and Technology Agency, Honcho 4-1-8, Kawaguchi 332-0012, Japan*
(Received 30 March 2008; revised manuscript received 9 July 2008; published 22 August 2008)

Subpicosecond time-resolved anisotropic transmission spectroscopy has been applied to one of the parent compounds of the colossal magnetoresistance manganites, orbital-ordered $LaMnO_3$, with and without the *A*-type antiferromagnetic order. $LaMnO_3$ is one of the simplest Mott insulators which facilitates unambiguous interpretation of the data. Two characteristic decay time constants are found; the fast one (τ_1) around 0.5 ps and the slow one (τ_2) around 10 ps. τ_1 is the same above and below T_N and is interpreted as the electron-phonon equilibration time. τ_2 shows very slight increase below T_N. We interpret τ_2 as the time constant for the orbital order to reach thermal equilibrium. The lack of a significant effect due to the magnetic order is explained using a recent band-structure calculation.

DOI: 10.1103/PhysRevB.78.075119 PACS number(s): 78.47.−p, 75.47.Lx

I. INTRODUCTION

Strongly correlated electron system, which shows variety of magnetic and electronic phases, is one of the hottest subjects in solid-state physics both from the fundamental and technical points of view.[1] The variety is derived from the competition between the spin, charge, and orbital degrees of freedom, which causes drastic changes in the electronic states triggered by external perturbation. For example, chemical doping into a Mott insulating cuprate induces high-T_C superconductivity, magnetic field applied to a charge-ordered insulator induces ferromagnetic metal [colossal magnetoresistance (CMR)] in manganites, and so on.

Photoirradiation is another powerful tool to induce a drastic change and a photoinduced phase transition has been reported in manganites.[2,3] The transition from a charge- and orbital-ordered (COO) insulator to a ferromagnetic (FM) metal has been studied by the femtosecond pump-and-probe (PP) reflection spectroscopy.[4] In a recent report on $Nd_{0.5}Sr_{0.5}MnO_3$, using the Kerr spectroscopy, it is observed that a FM state is induced from the antiferromagnetic (AFM) phase by photoirradiation.[5] A transient metallic state in $Gd_{0.55}Sr_{0.45}MnO_3$ was found to decay into the initial COO state within a few picoseconds.[6]

In an optical PP measurement, one monitors the change in the light intensity (reflectance or transmittance) and/or the polarization. The relevant physical properties studied by these measurements are usually the electronic structure and the magnetization, respectively. However, the electronic structure and the magnetism are not separable. Orbital also plays an important role in a PP measurement because it affects the electronic structure and birefringence as well; both intensity and polarization vary simultaneously. Therefore, in the previous studies mentioned above, unambiguous interpretation of the results is quite difficult. In order to simplify the situation and to facilitate the interpretation in a PP experiment, we chose one of the simplest Mott insulators $LaMnO_3$ for the current study.

$LaMnO_3$ is the parent compound of CMR manganites. The valence of the Mn ion is fixed at 3+, hence there is no charge degree of freedom. It exhibits $d_{3x^2-r^2}/d_{3y^2-r^2}$ orbital order of e_g electrons in the *ab* plane below T_{OO}(~780 K).[7] The same orbitals stack along the *c* axis. Below T_N(~140 K) (Ref. 8) the magnetic moments on Mn sites are aligned ferromagnetically in the *ab* plane and are stacked antiferromagnetically along the *c* axis (the *A*-type AFM order). Thus, by comparing the results above and below T_N, one can separate the spin dependent processes.

Anisotropic optical conductivity in $LaMnO_3$ was reported by Tobe *et al.*[9] [Fig. 1(b)], in which the optical anisotropy (the optical conductivity along the *ab* plane is higher than along the *c* axis) appears below T_{OO} and it changes gradually as the temperature is lowered without a dramatic change around T_N. This is quite unexpected, considering the extra energy cost of transferring electrons to a neighbor with an oppositely polarized core spin below T_N. The difficulty is resolved by a recent calculation,[10] which is also useful in interpreting the present PP data. The calculation and the interpretation will be presented in Sec. IV.

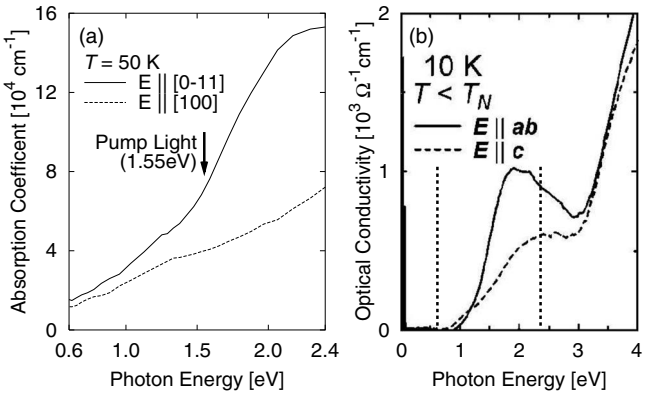

FIG. 1. (a) Anisotropic absorption spectra of a $LaMnO_3$ thin film on a LSAT (011) substrate at 50 K. The arrow shows the pump light energy used in this study. (b) Optical conductivity of a bulk $LaMnO_3$ reported by Tobe *et al.* (Ref. 9). Dotted vertical lines denote the energy range shown in (a).

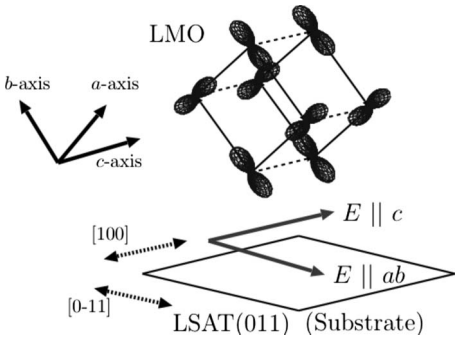

FIG. 2. Geometrical relationship between the orientation of the sample ($LaMnO_3$), the substrate [LSAT (011)], and the probe light polarizations.

II. EXPERIMENT

For a transmission measurement, we prepared a $LaMnO_3$ thin film, which was grown epitaxially by pulsed laser deposition technique on a $(LaAlO_3)_{0.3}(SrAl_{0.5}Ta_{0.5}O_3)_{0.7}$ (LSAT) (011) substrate, and the thickness was 100 nm. Since, with transmission, one can measure absorption which is directly connected to joint density of states, the data can be more simply interpreted than in a reflectance measurement.

From the XRD measurement and anisotropic absorption spectra (Fig. 1), it is revealed that the *ab* plane of $LaMnO_3$ is oriented along the $[0-11]$ axis of the substrate and the *c* axis along the [100] axis of the substrate, respectively (Fig. 2). The film structure allows us to monitor the electronic structure within the FM *ab* plane and that in the AFM *c* axis independently by selecting the probe light polarization. The structure is distinct from what has been ordinarily observed in a film on a (011) substrate[11,12] in which the *a* or *b* axis is along the [100] direction. This is because the lattice parameter of the substrate (3.87 Å) is closer to the length of the *c* axis of the $LaMnO_3$ (3.84 Å) than the length of the *a*,*b* axes (3.99 Å). The film is single domain and shows weak ferromagnetism as in a bulk crystal below T_N(=125 K).

For the time-resolved measurements, we used a Ti:sapphire regenerative amplifier system with a pulse width of 150 fs and repetition rate of 1 kHz. The data presented below were collected with the pump wavelength at 800 nm (1.55 eV) and the polarization was fixed to $E \| ab$ plane. No qualitative difference was found between the data taken with the pump polarization $E \| ab$ plane and those with $E \| c$ axis. This point will be discussed later. To probe the transmittance, we used light pulses from an optical parametric amplifier with the polarization $E \| ab$ plane or $E \| c$ axis. The energy of the probe light was in the range of 0.62–2.06 eV. To produce higher energy photons, the second harmonic was employed using a β-BaB_2O_4 crystal.

III. RESULTS

We first show the transient transmittance probed at 0.62 eV, which is in the energy gap. As shown in Fig. 3, for both polarization directions along the *ab* plane and along the *c* axis, the transmittance sharply decreases and recovers within 1 ps after the photoexcitation. This is the ultrafast metallization and decay similar to the results in a previous study.[6] The decay is due to the electron-phonon equilibration. After this ultrafast metallization, the transient transmittance decays anisotropically in some picoseconds at 7 K ($\ll T_N$). On the other hand, the decay is isotropic at 250 K ($\gg T_N$). The transmittance anisotropy $(dT/T_{[ab]} - dT/T_{[c]})$ at given times after pump is shown in Fig. 4(c), which clearly shows temperature dependence similar to that of the magnetization [Fig. 4(a)]. On the other hand, the static optical anisotropy estimated from the effective number of electrons N_{eff} $(\propto \int_{0.6\ \mathrm{eV}}^{2.4\ \mathrm{eV}} \sigma(\omega) d\omega)$ has no sudden change around T_N [Fig. 4(b)]. Here, the index of refraction needed to convert absorption into $\sigma(\omega)$ was assumed to be isotropic. Note that the main fraction of the anisotropy grows in the time scale of $5 \sim 10$ ps.

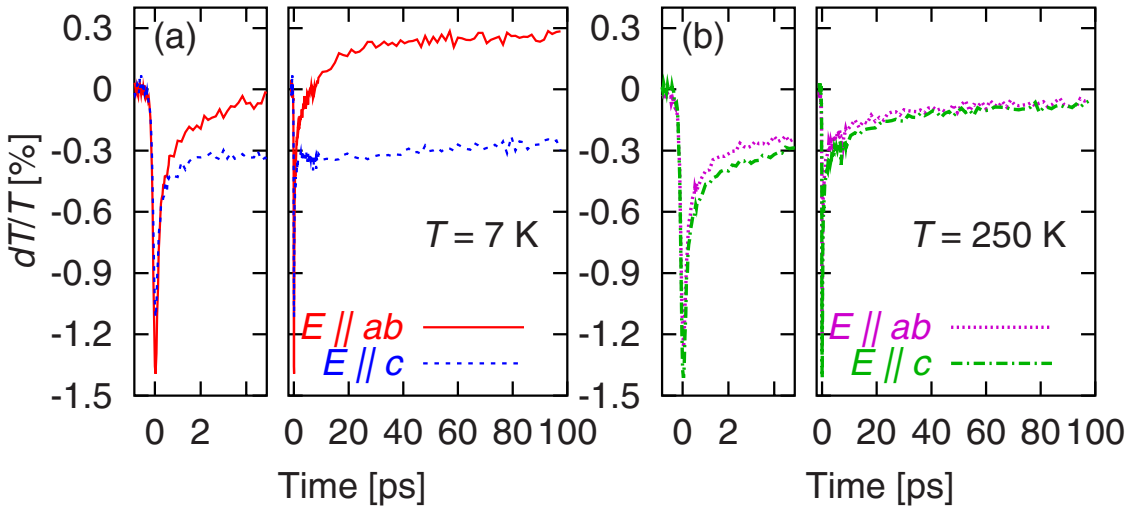

FIG. 3. (Color online) Transient differential transmittance probed at 0.54 eV with polarizations along the *ab* plane and the *c* axis, respectively. The pump intensity was 1.2 $\mathrm{mJ/cm^2}$ and the wavelength 800 nm. (a) is at 7 K ($\ll T_N$) and (b) is at 250 K ($\gg T_N$). The panel on the left of each figure is a magnification near $t=0$.

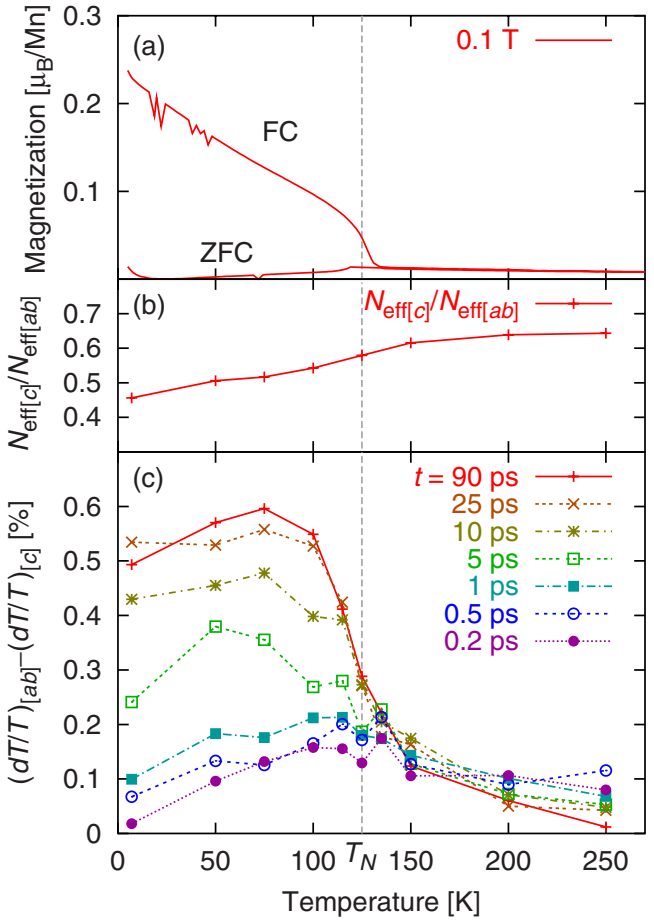

FIG. 4. (Color online) (a) Temperature dependence of magnetization. FC: field cooled, ZFC: zero-field cooled. (b) Optical anisotropy estimated from absorption spectra. N_{eff} is the effective number of electrons (see text). (c) Differential transmittance anisotropy at several elapsed times after photoexcitation.

In our earlier study,[5] we found a growth of a FM order after the destruction of the COO-AFM state. In order to see if the anisotropic response below T_N is related to the appearance of photoinduced FM order, we studied the polarization rotation (Faraday rotation) at 0.62 eV under magnetic fields up to 1 T. We found no sign of the polarization rotation (Fig. 5). The lack of the net photoinduced magnetization is understood in terms of the charge-transfer (CT) excitation allowed in the band structure (see below).

We further studied the transient transmittance spectra. The measured energy region is from 0.62 to 2.06 eV (below and above the energy gap). The measurements were done at 75 and 150 K. From the temperature dependence shown in Fig. 4(c), it is clear that the sample is deep in the AFM state at 75 K and well in the nonmagnetic state at 150 K. The results are shown in Fig. 6.

We analyzed the results by using a phenomenological three temperature model similar to that used to account for the thermalization of ferromagnetic metal.[13] The three temperatures in our case are the electron temperature T_e, the phonon temperature T_p, and the "orbital" temperature T_o. Various physical parameters, especially the specific heat due to each degree of freedom, are necessary to numerically

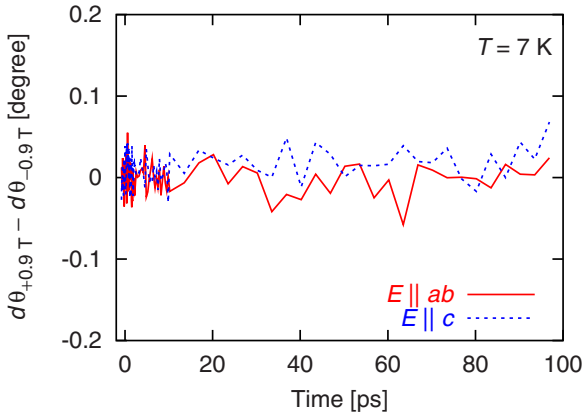

FIG. 5. (Color online) Faraday rotation after the pump at 7 K. The probe is at 0.62 eV. The difference of the polarization rotation taken at 0.9 and −0.9 T is plotted. Solid line shows the data for the probe polarization $E \| ab$ plane, and dashed line $E \| c$ axis.

solve the model. However, it can be shown that as long as the thermalization of the three degrees of freedom is temporally well separated (i.e., $\tau_1 \ll \tau_2 \ll \tau_3$, below), the optical response after the photoexcitation can be expressed as

$$f(t) = A_1 \exp(-t/\tau_1) + A_2 \exp(-t/\tau_2) + A_3 \exp(-t/\tau_3), \tag{1}$$

convoluted with the pulse-shape function. Here, A_i's are the functions of the probe energy. Numerically, as shown below, $\tau_1 \sim 0.5$ ps, $\tau_2 \sim 10$ ps, and $\tau_3 \sim 400$ ps, so that the premise is valid. In this model, as noted earlier, τ_1 is the electron-phonon equilibration time. This is a typical time scale of the electron-phonon interaction for wide range of solids.[14] After the electron and lattice equilibrates, the collective Jahn-Teller (J-T) distortion slowly reaches thermal equilibrium with the time constant τ_2. The degree of freedom that reflects the collective J-T distortion in the optical properties is the orbital, hence we denote the temperature T_o, but in reality it is a particular electron-phonon coupled mode. We will discuss about it later.

τ_3 is assigned as the thermal diffusion time from the sample to the substrate. This can be confirmed numerically by solving one-dimensional thermal diffusion equation

$$\frac{\partial T}{\partial t} = K \frac{\partial^2 T}{\partial x^2}. \tag{2}$$

Inserting published data $K = \kappa/\rho c$, $c = 5$ J/K mol,[15,16] and $\kappa = 0.1$ W/cm K (Ref. 17) for $LaMnO_3$ and $K = 0.0133$ cm^2/s (Ref. 18) for the substrate, LSAT, we find that the decay time constant of the sample average temperature is about 350 ps, in accordance with the observation.

The assumption that τ_3 is the thermal diffusion time constant to the substrate and there is no further relaxation process left (including the spin degree of freedom) is further confirmed by comparing the amplitude A_3 with the temperature dependence of the transmittance spectra. In Fig. 7, we show that A_3 spectra are well reproduced by the difference of the transmittance spectra taken at 100 and 75 K, and 200 and 150 K multiplied by a factor of 0.7. This indicates that the

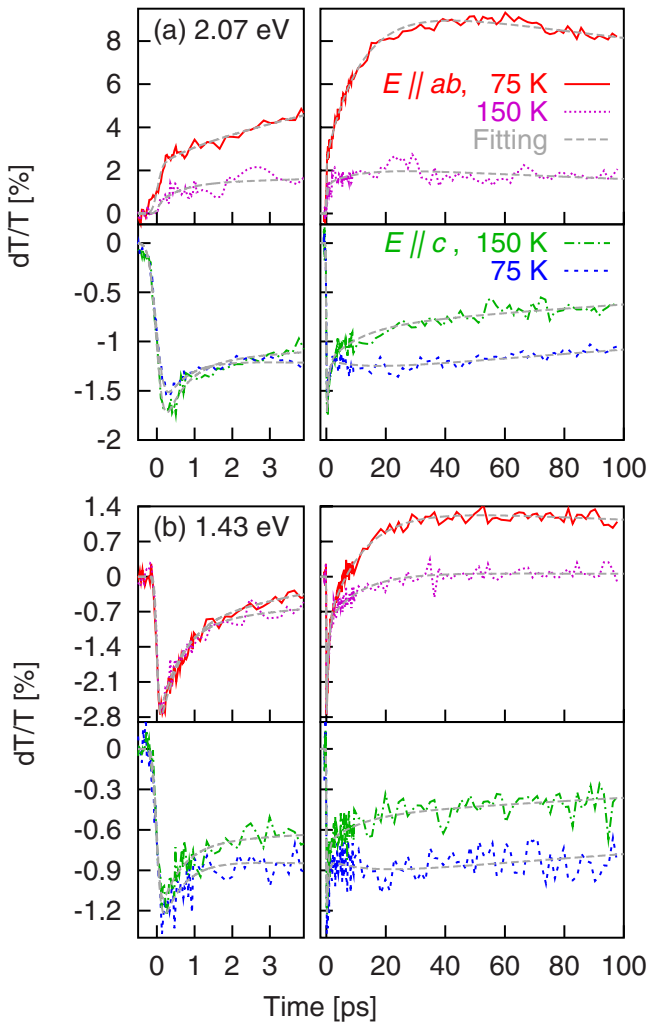

FIG. 6. (Color online) Transient differential transmittance for different temperature and probe polarizations at 2.06 and 1.43 eV. Gray long-dashed lines show the results of the fittings.

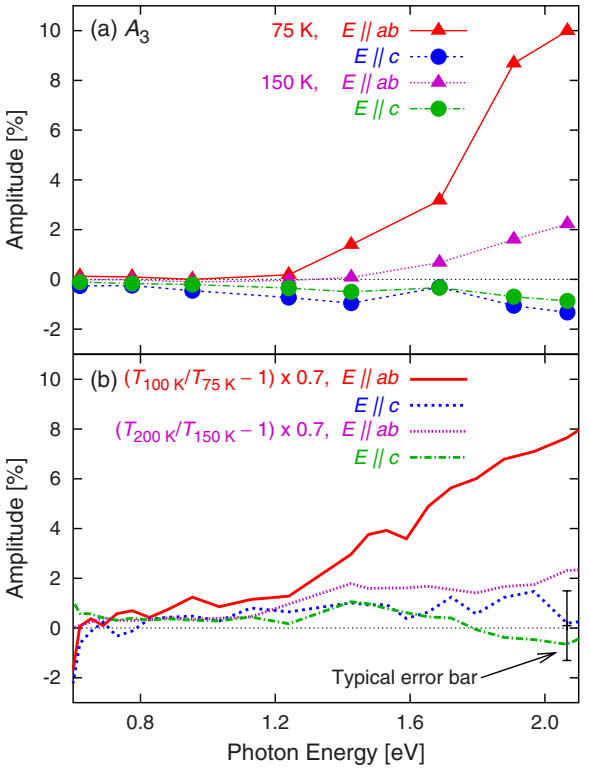

FIG. 7. (Color online) (a) Spectra of the amplitude of the slowest component (A_3), and (b) differential transmittance derived by varying the temperature. Each figure shows spectra with probe polarizations along the *ab* plane and along the *c* axis, and for $T<T_N$ and $T>T_N$.

sample is in complete thermal equilibrium during this period. The temperature rise by the photoexcitation is estimated to be about $25-50\times0.7\sim20-35$ K, which is similar to the earlier report on thin films under similar experimental conditions.[5]

The actual fitting process of the parameters A_i's and τ_i's to the experimental data was performed with a common set of τ_i's at each temperature; for a set of data with the same initial state and pump conditions, all data with different probe energy and polarization should share the same set of τ_i's if the probed states are considered equilibrium states of the subsystems (such as in the three temperature model). This assumption is verified with the quality of the fit, which, in our case, holds well as seen in Fig. 6.

Other results of the fitting are summarized in Fig. 8. The fitted time constants are $\tau_1=0.58\pm0.02$ ps, $\tau_2=11.9\pm0.2$ ps, and $\tau_3=490\pm24$ ps at 75 K, and $\tau_1=0.58\pm0.02$ ps, $\tau_2=10.9\pm0.4$ ps, and $\tau_3=305\pm19$ ps at 150 K. They are strikingly temperature insensitive aside from τ_3, whose temperature dependence is understood as the improved thermal conductivity in the film at a higher temperature. Since the electron-phonon interaction should not depend on the core spin order, the behavior of τ_1 is reasonable. The lack of significant change in τ_2 will be discussed in Sec. IV.

IV. DISCUSSION

In the model function Eq. (1), the sum $A_1+A_2+A_3$ represents the instantaneous electronic response. The overall photoinduced electronic response shown in Fig. 8(a) is summarized as (1) the spectral weight shift to lower energy in the *ab* plane and (2) the reduction of anisotropy. This behavior is natural, since, in the limit of heavy photoexcitation, the Mott gap should disappear resulting in an isotropic metal. The slight difference in the spectra at 75 and 150 K is due to the shift of the absorption edge to the lower energy at the lower temperature.

In our sample, two types of orders are the result of electron correlation; the orbital order and the AFM order. The presence of τ_2 above T_N and its insignificant change across T_N suggest that τ_2 is related to the orbital order. Considering that the orbital order is firmly connected to the lattice distortion and that the decay time of the photoinduced lattice distortion in manganites is in the range of 10 ps,[19] the assignment of the τ_2 process to the recovery of the Jahn-Teller lattice distortion after the photoexcitation is reasonable. However, the mystery is that there seems to be no additional

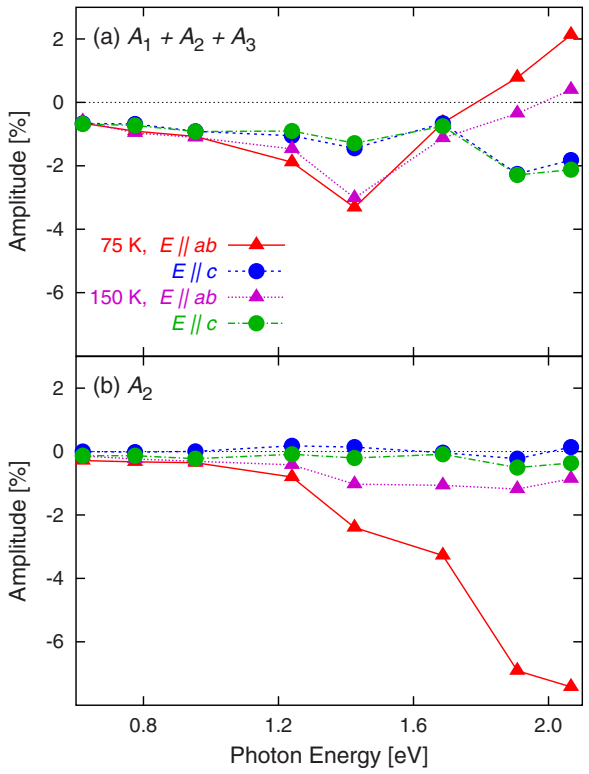

FIG. 8. (Color online) Probe energy dependence of the fitted amplitudes (a) $A_1+A_2+A_3$ and (b) A_2. Each figure shows spectra with probe polarizations along the *ab* plane (triangles) and along the *c* axis (circles), and for $T<T_N$ and $T>T_N$.

time constants necessary for fitting the data that reflects the magnetic order. This is understood in terms of the results of a recent theoretical calculation[10] mentioned in Sec. I.

The theory shows that, in the AFM state, the $d_{y^2-z^2\uparrow}$ orbital and the $d_{3x^2-r^2\downarrow}$ are both 1–2 eV above the ground state $d_{3x^2-r^2\uparrow}$. Here, arrows indicate the spin directions of the e_g electrons. Therefore, the energy needed to cause the optically-allowed and spin-conserving CT excitation in the *ab* plane is similar to that along the *c* axis. This can be easily seen as follows (Fig. 9). By denoting a Mn site by (i,j,k) in the a,b,c coordinate, the CT excitation along the AFM-ordered *c* axis occurs from the occupied $d_{3x^2-r^2\uparrow}(i,j,k)$ to the unoccupied $d_{3x^2-r^2\uparrow}(i,j,k\pm1)$ (not shown in Fig. 9), the energy cost of which is similar to the intralayer transition between the occupied $d_{3x^2-r^2\uparrow}(i,j,k)$ and empty $d_{z^2-x^2\uparrow}(i\pm1,j,k)$ [transition (a) shown in Fig. 9]. The core spin orientation, therefore, does not affect the transition energy very much. This explains why the optical properties change smoothly around T_N as noted in Sec. I.

The fact that the spin order does not affect the optical transition naturally implies that the optical transition does not disturb the spin order. The only signatures of the AFM order in the PP experiment are (1) the slight increase in τ_2 and (2) enhanced anisotropy exemplified in Fig. 4 and clearly shown in Fig. 8(b) in the behavior of A_2 at the low temperature. Note that A_2 is the amount of the contribution of the physical process associated with τ_2 to the optical absorption. Both can be explained again using Fig. 9.

After the photoexcitation within the *ab* plane (the FM ordered layer) from $d_{3x^2-r^2\uparrow}(i,j,k)$ to $d_{z^2-x^2\uparrow}(i+1,j,k)$ orbital

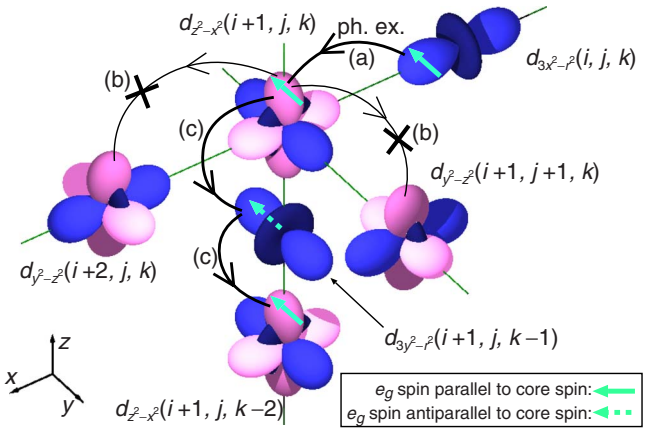

FIG. 9. (Color online) Orbital configuration of the photoexcited states in $LaMnO_3$. (a) CT photoexcitation along the *ab* plane. (b) Negligible transition along the *ab* plane, and (c) allowed transition along the *c* axis after the photoexcitation.

[transition (a) in Fig. 9], the excited electron can de-excite in a reverse process but cannot readily jump further to the empty $d_{y^2-z^2\uparrow}(i+2,j,k)$ or $d_{y^2-z^2\uparrow}(i+1,j\pm1,k)$ orbitals because the transfer integral is negligible [(b) in Fig. 9] due to the orbital symmetry. The orbital disorder would promote further transfer and gain in the kinetic energy. Photoexcitation thus can disturb the orbital order. On the other hand, the energy of the excited $d_{z^2-x^2\uparrow}(i+1,j,k)$ orbital is nearly degenerate (within ~0.5 eV) with that of the $d_{3y^2-r^2\uparrow}(i+1,j,k\pm1)$ orbital of the unoccupied spin in the neighboring layers. Therefore, there is a FM conduction band along the *c* axis and the excited electrons are mobile in the *c* direction [(c) in Fig. 9] without interfering with the spin or orbital orders. Note the asymmetry in the behavior of the CT transferred carriers (in the *ab* plane vs along the *c* axis) described above does not apply in the nonmagnetic state.

By acting on the orbital through the restricted CT transfer imposed by the spin order, the photoexcitation can reduce the in-plane orbital order and make it more metallic, causing the two characteristics (slightly enhanced τ_2 and much increased anisotropy in A_2) noted above. Note also that the motion of the electrons, either in the *ab* plane or along the *c* axis, does not interfere with the background AFM order. No net magnetization is anticipated as the result of the photoexcitation, which is in accordance with the experimental observation.

Long-range FM order usually produces long-lasting (more than hundreds of ps) effects after the photoexcitation.[20,21] The photoexcitation in the long-range AFM order, on the other hand, is short lived and is rather complex because it depends on the detailed electronic structure in the excited levels and hence is material dependent. This has been reiterated in a recent review.[22]

The model can also explain why the result is qualitatively independent of the polarization of the pump light. Although the initial electron-hole pair in the CT excitation depends on the polarization, the electron belongs to the same FM band in the excited level independent of the excitation process. The relaxation process afterwards is therefore indistinguishable; the electron-hole recombination rate may differ of course but is much faster than the temporal resolution of our setup.

V. CONCLUSION

We performed pump-and-probe transmittance spectroscopy on one of the simplest Mott insulators $LaMnO_3$. The orbital order, coupled to the lattice through Jahn-Teller effect, has a relatively long decay time constant of the order of 10 ps. The AFM order has a minimal effect to the decay constants because the CT excitation is compatible with the background AFM order and thus does not cause any disturbance to the magnetic order, whereas the photoexcitation usually perturbs the FM order very much leaving a long-lasting effect. The optical properties are explained using a recent numerical calculation.

ACKNOWLEDGMENTS

We thank T. Fujiwara and Y. Nohara for fruitful discussions on the numerical calculations of the model AFM ordered $LaMnO_3$. This work was supported by JSPS KAKENHI (Contract No. 19840014) and MEXT TOKUTEI (Contract No. 16076207).

*miyano@myn.rcast.u-tokyo.ac.jp

[1] Y. Tokura and N. Nagaosa, Science **288**, 462 (2000).
[2] K. Miyano, T. Tanaka, Y. Tomioka, and Y. Tokura, Phys. Rev. Lett. **78**, 4257 (1997).
[3] N. Takubo, Y. Ogimoto, M. Nakamura, H. Tamaru, M. Izumi, and K. Miyano, Phys. Rev. Lett. **95**, 017404 (2005).
[4] T. Ogasawara, K. Tobe, T. Kimura, H. Okamoto, and Y. Tokura, J. Phys. Soc. Jpn. **71**, 2380 (2002).
[5] K. Miyasaka, M. Nakamura, Y. Ogimoto, H. Tamaru, and K. Miyano, Phys. Rev. B **74**, 012401 (2006).
[6] Y. Okimoto, H. Matsuzaki, Y. Tomioka, I. Kezsmarki, T. Ogasawara, M. Matsubara, H. Okamoto, and Y. Tokura, J. Phys. Soc. Jpn. **76**, 043702 (2007).
[7] Y. Murakami, J. P. Hill, D. Gibbs, M. Blume, I. Koyama, M. Tanaka, H. Kawata, T. Arima, Y. Tokura, K. Hirota, and Y. Endoh, Phys. Rev. Lett. **81**, 582 (1998).
[8] E. O. Wollan and W. C. Koehler, Phys. Rev. **100**, 545 (1955).
[9] K. Tobe, T. Kimura, Y. Okimoto, and Y. Tokura, Phys. Rev. B **64**, 184421 (2001).
[10] Y. Nohara, A. Yamasaki, S. Kobayashi, and T. Fujiwara, Phys. Rev. B **74**, 064417 (2006).
[11] Y. Ogimoto, M. Nakamura, N. Takubo, H. Tamaru, M. Izumi, and K. Miyano, Thin Solid Films **486**, 104 (2005).
[12] M. Nakamura, Y. Ogimoto, H. Tamaru, M. Izumi, and K. Miyano, Appl. Phys. Lett. **86**, 182504 (2005).
[13] E. Beaurepaire, J.-C. Merle, A. Daunois, and J.-Y. Bigot, Phys. Rev. Lett. **76**, 4250 (1996).
[14] S. K. Sundaram and E. Mazur, Nat. Mater. **1**, 217 (2002).
[15] B. F. Woodfield, M. L. Wilson, and J. M. Byers, Phys. Rev. Lett. **78**, 3201 (1997).
[16] B. F. Woodfield, J. L. Shapiro, R. Stevens, and J. Boerio-Goates, Phys. Rev. B **60**, 7335 (1999).
[17] J. L. Cohn, J. J. Neumeier, C. P. Popoviciu, K. J. McClellan, and Th. Leventouri, Phys. Rev. B **56**, R8495 (1997).
[18] A. Stanimirovic, N. M. Balzaretti, A. Feldman, and J. E. Graebner, J. Mater. Res. **16**, 678 (2001).
[19] D. Lim, V. K. Thorsmølle, R. D. Averitt, Q. X. Jia, K. H. Ahn, M. J. Graf, S. A. Trugman, and A. J. Taylor, Phys. Rev. B **71**, 134403 (2005).
[20] A. I. Lobad, R. D. Averitt, C. Kwon, and A. J. Taylor, Appl. Phys. Lett. **77**, 4025 (2000).
[21] R. D. Averitt, A. I. Lobad, C. Kwon, S. A. Trugman, V. K. Thorsmølle, and A. J. Taylor, Phys. Rev. Lett. **87**, 017401 (2001).
[22] M. Fiebig, N. P. Duong, T. Satoh, B. B. Van Aken, K. Miyano, Y. Tomioka, and Y. Tokura, J. Phys. D **41**, 164005 (2008).